Supporting Information:

$P(CN)_3$ Precursor for Carbon Phosphonitride Extended Solids

Brian L. Chaloux[1,†], Brendan L. Yonke[1,†], Andrew P. Purdy[2], James P. Yesinowski[2], Evan R. Glaser[2], Albert Epshteyn[2,*]

[1] NRC Postdoctoral Associate, U.S. Naval Research Laboratory, Washington, DC 20375

[2] Chemistry Division, U.S. Naval Research Laboratory, Washington, DC 20375

[3] Electronics Science and Technology Division, U.S. Naval Research Laboratory, Washington, DC 20375

† These authors contributed equally to this work

* Corresponding author

SYNTHESIS

Materials. Phosphorus(III) chloride (98 %) was purchased from Alfa Aesar and used as received. Silver(I) cyanide (99 %) was purchased from Acros Organics and dried at elevated temperature under vacuum prior to use. Benzene (99.8 %, anhydrous) was purchased from Sigma–Aldrich and vacuum distilled from sodium–benzophenone ketyl prior to use. Deuterated acetonitrile (CD_3CN, 99 at. % D) was purchased from Cambridge Isotope Laboratories and dried over 4 Å molecular sieves prior to use.

***WARNING:* Phosphorus tricyanide hydrolyzes readily to toxic HCN in the presence of water and may combust violently in dry air.[1] Use of well-ventilated spaces is necessary when handling and disposing of $P(CN)_3$, and use of inert (argon or nitrogen) atmosphere is recommended whenever possible to minimize the chance of explosion or exposure to toxic gases. When stored under dry argon or nitrogen at room temperature, $P(CN)_3$ is stable indefinitely.**

Phosphorus tricyanide [$P(CN)_3$]. Phosphorus tricyanide was synthesized according to a literature procedure.[1] Phosphorus(III) chloride (3.469 g, 25.26 mmol) and silver(I) cyanide (10.487 g, 78.33 mmol) were added to 70 mL anhydrous benzene and the suspension was refluxed under N_2 for 16 h. Volatiles were removed from the resulting grey slurry under vacuum and the crude solid product was sublimed twice at 120 °C under dynamic vacuum, affording white, needlelike crystals in 92 % yield (2.534 g) which were qualitatively pure by NMR and vibrational spectroscopy. ^{13}C NMR (CD_3CN, 75 MHz): δ = 111.67 (d, $^1J_{C\text{-}P}$ = 60.0 Hz) ppm. ^{31}P NMR (CD_3CN, 121 MHz): δ = -138.71 (s + d, $^1J_{C\text{-}P}$ = 60.0 Hz) ppm. IR: ν = 2205 m, 632 vs, 602 vs, 574 vs, 466 vw, 451 vw cm^{-1}. Raman: ν = 2205 vs, 632 m, 602 m, 574 m, 466 m, 451 w, 314 w, 155 s, 147 s, 119 s cm^{-1}.

The melting point of $P(CN)_3$ was previously reported as 200 °C and formation of a black solid at this temperature was noted in the literature.[1,2] In attempting to observe the melting point of $P(CN)_3$, our own experiments showed that it darkened substantially when slowly heated to temperatures as low as 180 °C in sealed capillaries, whereas only sintering was observed above 200 °C.[3-6] Actual melting to a pale yellow liquid was observable at 205–210 °C only when capillaries were inserted into a preheated apparatus – the liquid blackening and solidifying while holding at temperature. Self-reaction of $P(CN)_3$ appeared to occur even in the solid state, with discoloration apparent at 25–30 °C below its melting point.

$C_3N_3PO_{1-x}$. Phosphorus tricyanide (0.622 g) was powdered, loaded into a thick-walled Pyrex tube flame sealed on one end, and evacuated. The open end was subsequently flame sealed under vacuum. The sealed tube containing $P(CN)_3$ was heated in a box furnace to 220 °C for 16 h, quickly changing from a white powder to a black solid via a short-lived solid, red-orange, intermediate. After slow cooling to room temperature, the tube was broken and the black solid (0.613 g) isolated under inert atmosphere in 98.6 % yield based on the mass of $P(CN)_3$. This solid was transferred to a vial under argon, removed from the glove box, opened, and exposed to air; no immediate

change in mass was observed. After 16 hours of air exposure, the product was weighed, degassed, transferred to the glove box, and re-weighed under argon at 0.645 g (+ 5.2 % mass). The calculated increase in mass was the same under argon and under air to within 0.1 %. No subsequent change in mass was observed after an additional 72 hours of air exposure. IR: ν = 3170 s + br, 1550 s, 1380 m, 1210 s, 990 m, 580 w cm^{-1}. Raman: ν = 3040 s + br, 2230 vw, 1530 s, 1390 m + br, 1050 vw, 800 w, 720 w, 650 w + br, 440 w, 350 w cm^{-1}. ^{13}C NMR (neat, 126 MHz): δ = 180 – 100 (broad), 114 ppm. ^{31}P NMR (neat, 202 MHz): δ = 227, -3 ppm.

CHARACTERIZATION METHODS

Infrared (IR) spectra were acquired on a Nicolet iS50 FT-IR spectrometer. Transmission spectra of $P(CN)_3$ crystals were acquired by drop casting $P(CN)_3$ from dilute solution in diethyl ether onto NaCl plates at room temperature. Attenuated total internal reflectance (ATR) spectra of $C_3N_3PO_{1-x}$ were acquired on a diamond crystal. Spectra were referenced to bare NaCl plates and diamond ATR crystal, respectively, and corrected with linear, 2-point baselines. Raman spectra were acquired on a Renishaw inVia confocal Raman microscope using an argon ion laser operating at 514 nm; no background subtractions were performed. The spectra of $P(CN)_3$ synthesized as described are depicted in Figure S1 and the corresponding peak assignments (from literature) given in Table S1. The partial derivative character of the IR spectra of both $P(CN)_3$ (Figure S1) and $C_3N_3PO_{1-x}$ (Figure 4) is due to reflectance character in the transmission spectra due to scattering from large crystallites of $P(CN)_3$ and in the ATR spectra due to poor contact of the hard $C_3N_3PO_{1-x}$ powder with the diamond ATR surface. The poor contact between $C_3N_3PO_{1-x}$ and the IR crystal also gives rise to low signal-to-noise. Attempts to prepare KBr pellets of $C_3N_3PO_{1-x}$ to overcome the difficulties associated with ATR measurements resulted only in opaque discs after pressing, due to coalescence of the black, micron-sized $C_3N_3PO_{1-x}$ particles under shear.

Nuclear magnetic resonance (NMR) spectra for solutions were acquired on a Bruker Avance 300 spectrometer operating at 75 MHz for ^{13}C and 121 MHz for ^{31}P. ^{13}C chemical shifts were referenced to TMS using CD_3CN as a secondary chemical shift reference at 7.24 ppm and ^{31}P chemical shifts to an external 85% H_3PO_4 standard. Magic angle spinning (MAS) NMR experiments were carried out on a Varian/Agilent DDRS 11.7 T NMR spectrometer using a 3.2 mm triple-resonance probe operating at 126 MHz for ^{13}C and 202 MHz for ^{31}P. The ^{13}C and ^{31}P chemical shifts were referenced using a secondary reference of adamantane[7] and to a 85% phosphoric acid standard, respectively. Rotor-synchronized 90^0 - τ - 180^0 - τ – acquire Hahn-echo pulse sequences were used with τ = 55.6 μs in order to obtain flat baselines for the broad peaks. For ^{13}C the 90° pulse length was 2.2 μs and the relaxation delay was 100 s (a shorter delays of 10 s produced only modest changes in relative intensities of the peaks). For ^{31}P the 90° pulse length was 1.2 μs and the relaxation delay was 10 s. The ^{31}P spectra were acquired at spinning rates of 18.0 kHz and 25.0 kHz to identify spinning sidebands, with the lower spinning speed having less overlap of sidebands from the two peaks. Figure 6 shows the ^{31}P MAS-NMR spectrum and Figure S2 the ^{13}C MAS-NMR spectrum (13-day accumulation time) of $C_3N_3PO_{1-x}$ acquired at spinning rates of 18.0 kHz. Electron spin resonance (ESR) spectra (Figure S9) were acquired using a commercial (E-300) Bruker spectrometer operating at a frequency of 9.51 GHz. X-ray photoelectron spectra (XPS, Figure S3) were collected on a Thermo Scientific K-Alpha XPS. Binding energies were calibrated to adventitious carbon (C1s = 284.8 eV). Spectra were fit with Shirley backgrounds and symmetrical, 70% Gaussian–30% Lorentzian (GL) peaks.

Skeletal densities were measured using a Micromeritics AccuPyc 1330 helium pycnometer. Brunauer–Emmett–Teller (BET) N_2 adsorption measurements were made using a Micromeritics ASAP 2020 physisorption analyzer at a temperature of 77 K (Figure S4). Samples were degased at 200 °C under vacuum for 4 hours prior to analysis. Scanning electron microscope (SEM) images were collected on a Leo SUPRA 55 field emission SEM operating at 5 keV (Figure S5). Energy dispersive spectra (EDS) of the associated SEM images (Figure S6) were collected using a Princeton Gamma-Tech PRISM 2000 digital spectrometer at an SEM operating voltage of 20 keV.

X-ray diffraction patterns were acquired on a Rigaku SmartLab X-ray diffractometer using Cu K_α radiation (Figure S7). Transmission electron microscopy (TEM) was performed on a JEOL 2200FS equipped with a Gatan Ultrascan charge coupled device (CCD) camera (Figure S8).

Thermal gravitational analysis (TGA) was performed in alumina pans on a TA Instruments SDTQ600 TGA-DTA at a heating rate of 10 °C min^{-1} under 100 mL min^{-1} N_2 (7.7 mg) and air flow (5.3 mg) (Figure 3). $C_3N_3PO_{1-x}$ powder was used as isolated, without further processing, resulting in particles 1–100 μm in diameter. An irregular loss of mass at ~800 °C likely corresponds to physical ejection of particulate from the open alumina pans due to buildup of internal pressure, causing fracture of the powder. Melting points were determined on an Electrothermal melting point apparatus using 1.5 mm glass capillaries packed under inert atmosphere and subsequently flame-sealed.

SUPPLEMENTAL FIGURES AND TABLES

Table S1. Vibrational modes of $P(CN)_3$[8,9,this work]

ν (cm^{-1})	*symmetry*	*activity*	*intensity*[†]	*description of mode*
2205	$A_1 + E$	IR, R	s, vs	C≡N stretch
632, 602	A_1	IR, R	vs, m	P-C stretch (Fermi resonant w/ PC_3 + P-C≡N comb. band)
574	E	IR, R	s, m	P-C stretch
466	A_1	IR, R	vw, m	P-C≡N bend
451	E	IR, R	vw, w	″ ″
314	E	IR, R	w[‡], w	″ ″
155	E	IR, R	m[‡], s	PC_3 deformation
147	A_1	IR, R	s[‡], s	″ ″
119	–	–	w[‡], s	lattice phonon (not obs. in sol'n)

[†] vw = very weak, w = weak, m = medium, s = strong, vs = very strong

[‡] below frequency cutoff used for IR measurements; based on literature

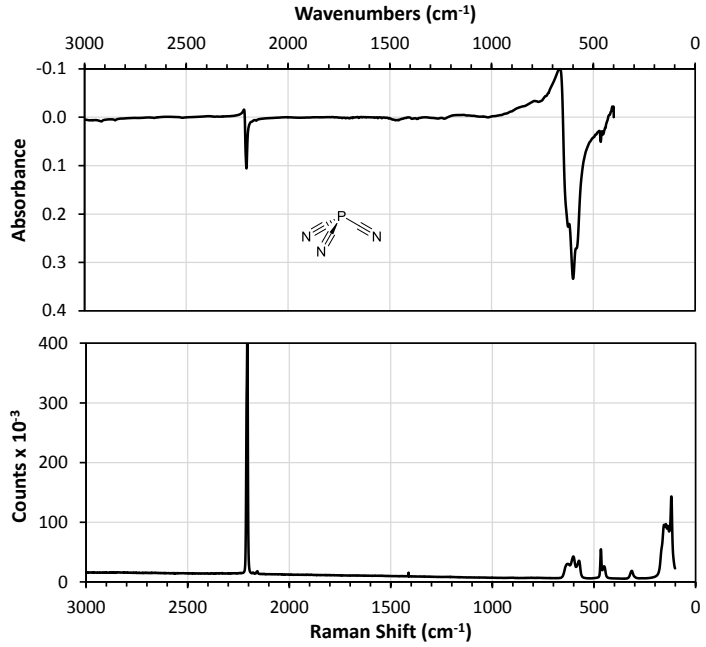

Figure S1. FT-IR (top) and Raman (bottom) spectra of neat $P(CN)_3$, as synthesized according to the reported experimental procedure. See Table S1 for literature assignment of peaks.

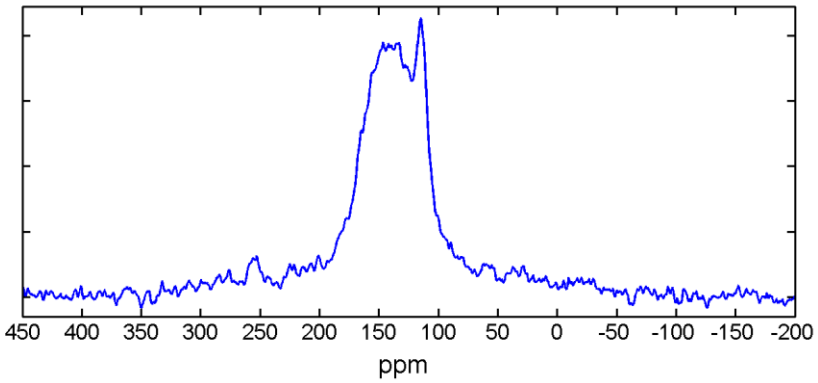

Figure S2. ^{13}C NMR spectrum of $C_3N_3PO_{1-x}$ under 18.0 kHz MAS.

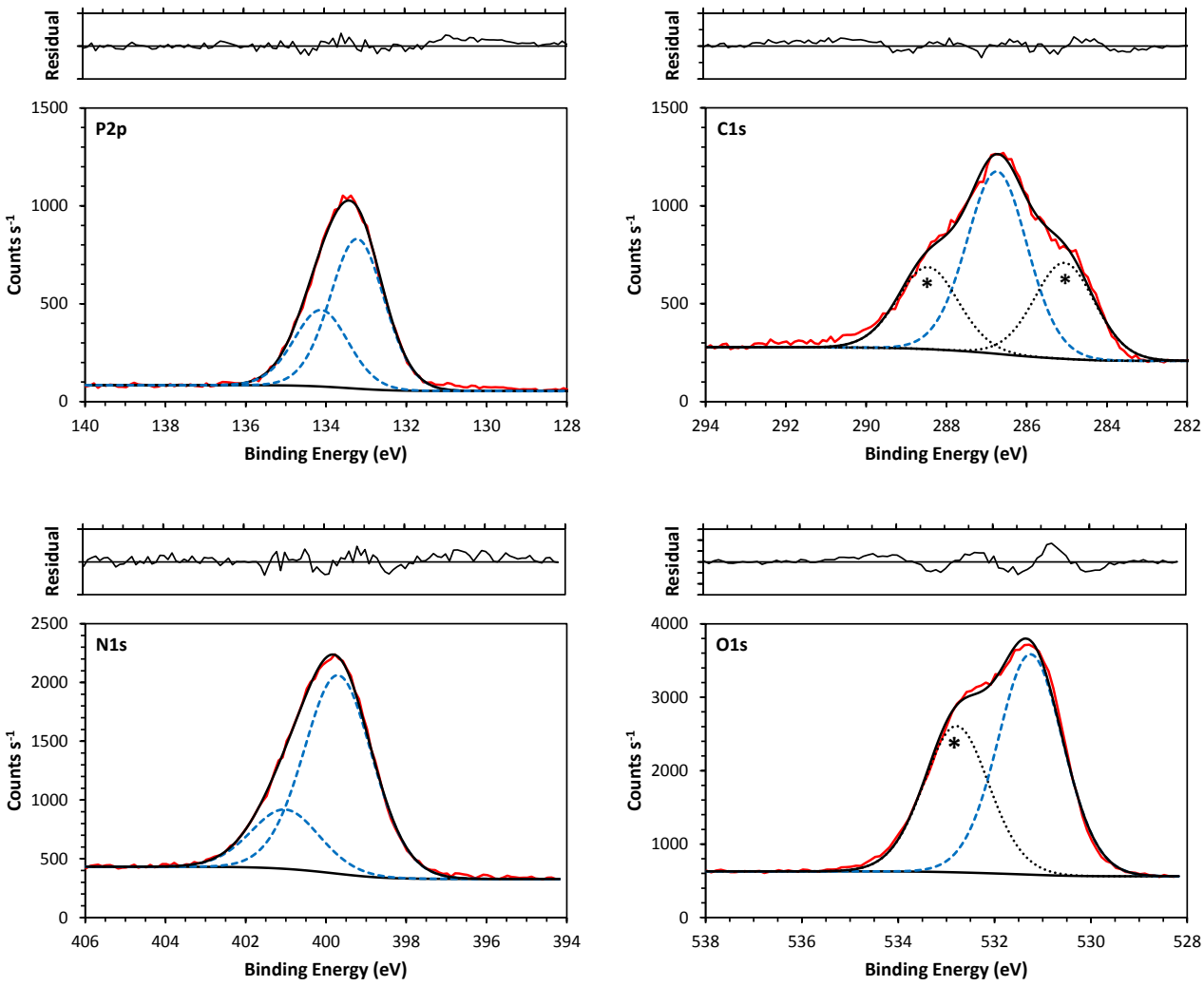

Figure S3. P2p, C1s, N1s, and O1s regions of the X-ray photoelectron spectrum of $C_3N_3PO_{1-x}$. Raw data in red and Shirley background, fit envelope, and residuals in black. Tick marks of residual axes are ± 100 counts s^{-1}. Peak fits corresponding to adventitious carbonaceous species are black, dotted lines marked with asterisks. Other peaks are fit with blue, dashed lines.

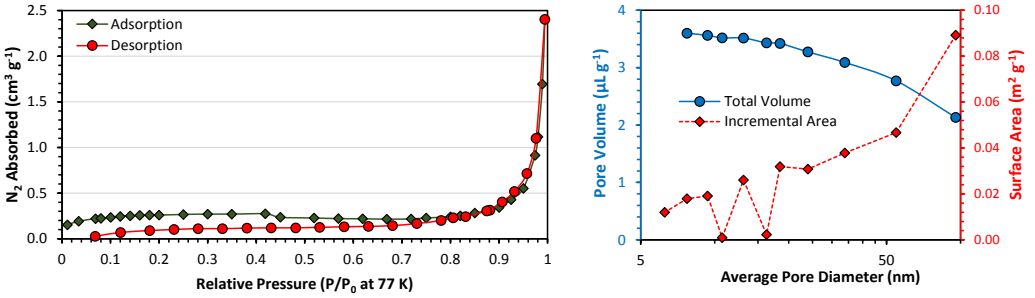

Figure S4. Left) N_2 adsorption and desorption curves for $C_3N_3PO_{1-x}$ at 77 K. Right) Pore volume and surface area calculated from Brunauer–Emmett–Teller analysis of desorption curve.

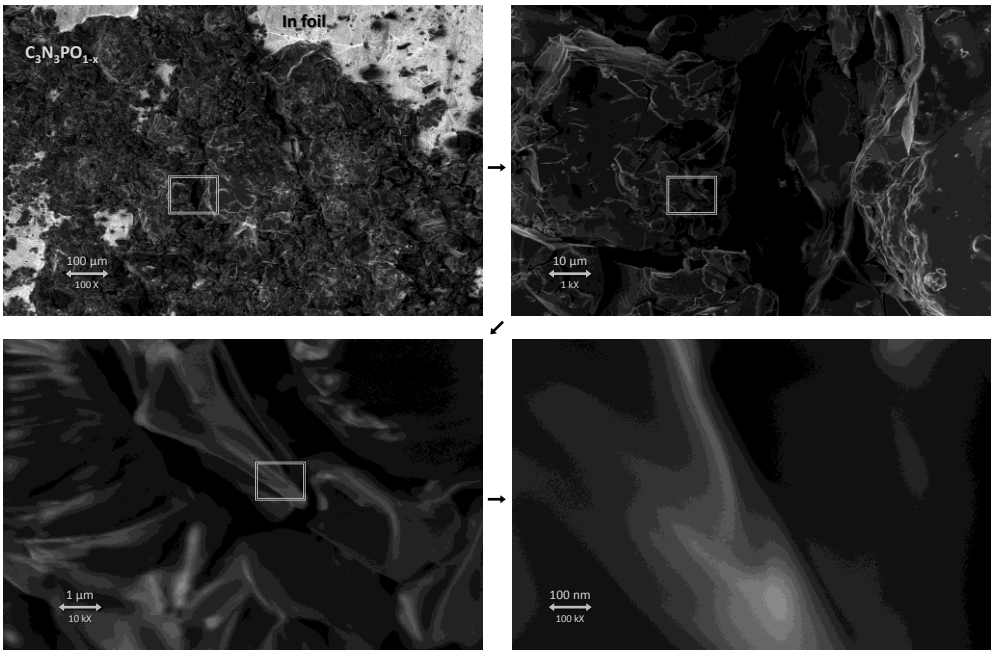

Figure S5. SEM images of $C_3N_3PO_{1-x}$ in indium foil at progressively higher magnification. Areas of magnified images are highlighted with grey boxes in images at lower magnification.

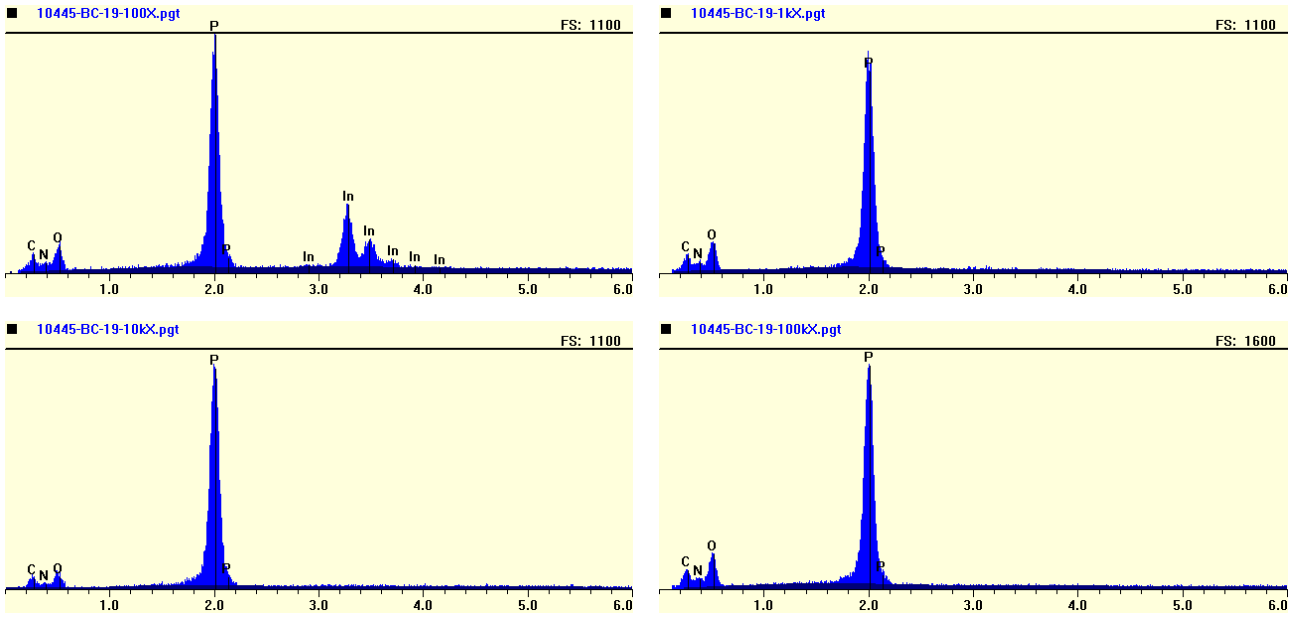

Figure S6. Energy dispersive x-ray spectra (EDS) from the $C_3N_3PO_{1-x}$ regions depicted in Figure S5. Bottom axes in eV.

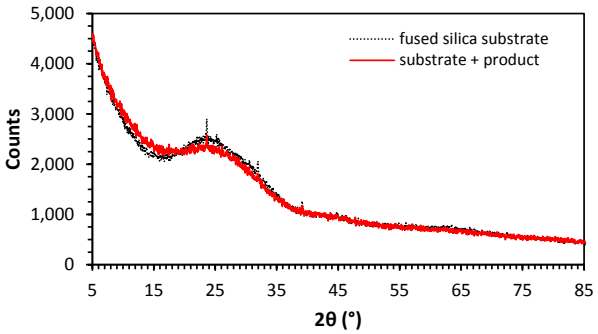

Figure S7. X-ray diffraction patterns of $C_3N_3PO_{1-x}$ particles (red) on fused silica and bare fused silica substrate (black).

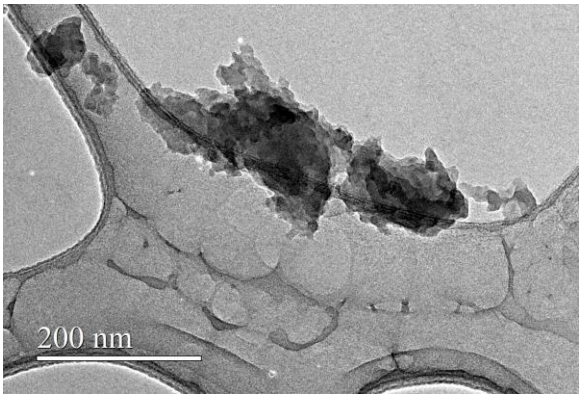

Figure S8. Transmission electron micrograph of as-synthesized $C_3N_3PO_{1-x}$, showing no discernible morphology.

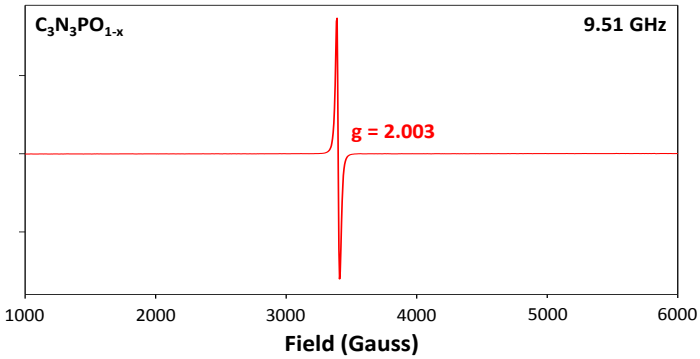

Figure S9. Wide scan ESR spectrum of 15 mg $C_3N_3PO_{1-x}$ (5 scans).

Table S2. Selected* vibrational modes of triphenylphosphine[10] / -oxide[11], melamine[12,13], an melem[14]

ν (cm^{-1})	*symmetry*	*activity*	*intensity*†	*description of mode*
			triphenylphosphine[10] / -oxide[11]	
1150	A_1	IR, R	s, vw	P=O stretch
705	E	IR, R	s, m	P-C stretch
683	A_1	IR, R	vw, s	″ ″
370	E	IR, R	nr, vw	P=O bend
299	A_1	IR, R	nr, vw	PC_3 deformation
256	E	IR, R	nr, m	″ ″
			melamine (1,3,5-triamino-*s*-triazine)[12,13]	
1598‡	E' (E)	IR, R	vs, vw	ring stretching + NH_2 scissoring
1560	E' (E)	IR, R	s, m	quadrant ring stretch
1440	E' (E)	IR, R	vs, w	semi-circle ring stretch
990‡	E' (E)	IR, R	m, s	substituent swing (N-C-NH_2)
920	(A_1)	(IR, R)	(vw, w)	N radial ring breathing
820	A_2'' (A_1)	IR, (R)	m, (vw)	out-of-plane ring deformation
750‡	E' (E)	IR, R	vw, w	″ ″
690‡	(A_1)	(IR, R)	(w, vs)	C radial ring breathing
580	E' (E)	IR, R	m, m	NH_2 + C-N-H bend
550‡	(E)	(IR, R)	(s, vw)	substituent swing (N-C-NH_2)
			melem (2,5,8-triamino-*s*-heptazine)[14]	
1677	E' + A_1'	IR, R	s, w	*unassigned*
1606	E'	IR, R	vs, m	
1581	E'	IR, R	s, w	
1547	A_1'	R	w	
1469	E'	IR, R	vs, m	
1396	A_1'	R	w	
1304	E'	IR, R	w, vw	
1155	E' + A_1'	IR, R	w, s	
1068	E'	IR, R	m, vw	
938	E'	IR, R	vw, m	
802	A_2''	IR	s	
745	A_1' + A_2''	IR, R	vw, m	
531	A_1'	R	vs	
449	E'	IR, R	s, m	

* phosphine / -oxide: all P-C and P=O modes; melamine: all active ring modes (low symmetry conformer)

† vw = very weak, w = weak, m = medium, s = strong, vs = very strong, nr = not reported

‡ frequency of mode coupled to mass of ring substituents

REFERENCES FOR SUPPORTING INFORMATION

(1) Staats, P. A.; Morgan, H. W.; Cohen, H. M. In *Inorg. Synth.*; Rochow, E. G., Ed.; John Wiley & Sons, Inc.: Hoboken, NJ, USA, 1960; Vol. 6, p 84.

(2) Emerson, K.; Britton, D. *Acta Crystallographica* **1967**, *23*, 506.

(3) Wehrhane, G.; Hübner, H. *Annalen der Chemie und Pharmacie* **1864**, *132*, 277.

(4) Goubeau, J.; Haeberle, H.; Ulmer, H. *Zeitschrift für anorganische und allgemeine Chemie* **1961**, *311*, 110.

(5) Bither, T. A.; Knoth, W. H.; Lindsey, R. V.; Sharkey, W. H. *J. Am. Chem. Soc.* **1958**, *80*, 4151.

(6) Krolevets, A. A.; Martynov, I. V. *Zh. Obshch. Khim.* **1991**, *61*.

(7) Earl, W. L.; Vanderhart, D. L. *Journal of Magnetic Resonance (1969)* **1982**, *48*, 35.

(8) Jensen, J. O. *Spectrochimica Acta Part A: Molecular and Biomolecular Spectroscopy* **2004**, *60*, 2537.

(9) Miller, F. A.; Frankiss, S. G.; Sala, O. *Spectrochim. Acta* **1965**, *21*, 775.

(10) Pikl, R.; Duschek, F.; Fickert, C.; Finsterer, R.; Kiefer, W. *Vib. Spectrosc* **1997**, *14*, 189.

(11) Daasch, L. W.; Smith, D. C. *The Journal of Chemical Physics* **1951**, *19*, 22.

(12) Wang, Y.-L.; M. Mebel, A.; Wu, C.-J.; Chen, Y.-T.; Lin, C.-E.; Jiang, J.-C. *J. Chem. Soc., Faraday Trans.* **1997**, *93*, 3445.

(13) Liu, X. R.; Zinin, P. V.; Ming, L. C.; Acosta, T.; Sharma, S. K.; Misra, A. K.; Hong, S. M. *Journal of Physics: Conference Series* **2010**, *215*, 012045.

(14) Jürgens, B.; Irran, E.; Senker, J.; Kroll, P.; Müller, H.; Schnick, W. *J. Am. Chem. Soc.* **2003**, *125*, 10288.